Journal of Photochemistry and Photobiology A: Chemistry 227 (2012) 1–10

Contents lists available at SciVerse ScienceDirect

Journal of Photochemistry and Photobiology A: Chemistry

journal homepage: www.elsevier.com/locate/jphotochem

The effect of nitro substitution on the photochemistry of benzyl benozhydroxamate: Photoinduced release of benzohydroxamic acid

Whitney R. Grither, James Korang, Jacob P. Sauer, Matthew P. Sherman, Pamela L. Vanegas, Miao Zhang, Ryan D. McCulla*

Saint Louis University, Department of Chemistry, Monsanto Hall, 3501 Laclede Ave., St. Louis, MO 63103, United States

ARTICLE INFO

Article history:
Received 10 May 2011
Received in revised form
28 September 2011
Accepted 3 October 2011
Available online 18 October 2011

Keywords:
Hydroxamate
Nitroxyl
Nitrosyl hydride
Photolabile protecting group
Nitrobenzyl
Wavelength dependent

ABSTRACT

The redox congener of the important signaling agent nitric oxide (NO), nitroxyl or nitrosyl hydride (HNO) has also been demonstrated to induce distinct physiological effects. The aim of this study was to determine if benzohydroxamic acid, which was selected as a stable model compound of HNO donors, could be released by the *o*-nitrobenzyl photolabile protecting group (PPG) in a wavelength-dependent manner. It was expected that selective irradiation of the *o*-nitrobenzyl chromophore would favor the release of benzohydroxamic acid over undesired products associated with N–O bond cleavage. Quantum yields for the release of benzohydroxamic acid protected by the *o*-nitrobenzyl PPG increased at longer wavelengths, with a concomitant decrease in the yield of minor products. Through the use of triplet photosensitizers, triplet quenchers, computational methods, and the position of the nitro substituent, insights into the nature of the mechanism were suggested.

1. Introduction

The redox congener of the important signaling agent nitric oxide (NO), nitroxyl or nitrosyl hydride (HNO), has also been demonstrated to induce distinct physiological effects [1–5]. The therapeutic utilization of HNO has been used to inhibit aldehyde dehydrogenases (ALDH) in the treatment of alcoholism [6,7]. Recent efforts have focused on application of HNO in cardiovascular conditions, such as the treatment of congestive heart failure, atherosclerosis, and vascular thrombosis [8–13]. Additionally, HNO donors afforded neuroprotection from excitotoxic assault by down-regulating *N*-methyl-D-aspartate (NMDA) receptors [14]. Biological targets of HNO have been identified as thiols, transition metals, iron–sulfur clusters, and DNA [15–18].

The rapid dehydrative dimerization of HNO to nitrous oxide and water necessitates in situ generation to investigate the chemistry and underlying biochemistry of HNO [19,20]. As shown in Scheme 1, the exogenous generation of HNO can be achieved through the decomposition of HNO donors such as Angeli's salt (NaN_2O_3) and Piloty's acid ($PhSO_2NOH$) [21]. However, release of HNO from these donors depends upon the spontaneous degradation of the donors, which is not a controlled event. To provide better spatial and temporal control over the generation of HNO, several investigators have examined methods of photochemically generating HNO in solution. Acyl nitroso compounds undergo hydrolysis to release HNO, and adducts between 9,10-dimethylanthracene and acyl nitroso derivatives have been photoinduced to undergo a retro-Diels–Alder reaction that releases the acyl nitroso HNO donor [22]. The photo-induced fragmentation of 3,5-diphenyl-1,2,4-oxadiazole-4-oxide produces an acyl nitroso intermediate whose decomposition also releases HNO [23]. However, these methods either require aqueous insoluble reagents or incident wavelengths that are absorbed by biomolecules, which often leads to photodamage and phototoxicity. Photolabile protecting groups (PPG) afford researchers exquisite spatial, temporal, and concentration control of the release of bioactive agents at wavelengths that induce little photodamage [24,25]. A seemingly straightforward strategy to generate HNO would be to protect a HNO donor with a PPG. Upon photolysis, the caged HNO donor would be liberated. In addition, this could lead to more rapid generation of HNO due to residual vibrational energy carried over from the initial excitation.

A potential complicating factor facing the release of an organic based HNO donor caged by a PPG is that they contain bonds that are potentially photosensitive. For example, *N*,*O*-diacylhydroxylamines, hydroxamic acids, and *N*-alkylbenzohydroxamates have all been shown to undergo N–O bond homolysis upon irradiation [26–31]. Alkyl benzohydroxamates undergo triplet state Norrish Type II photoelimination to

* Corresponding author. Tel.: +1 314 977 2850.
E-mail address: rmccull2@slu.edu (R.D. McCulla).

1010-6030/$ – see front matter © 2011 Elsevier B.V. All rights reserved.
doi:10.1016/j.jphotochem.2011.10.005

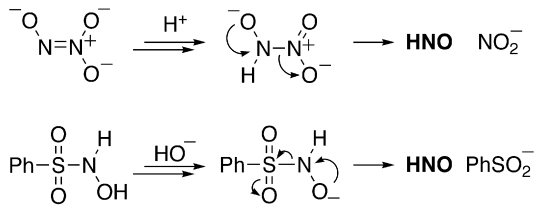

Scheme 1.

produce benzamide and the corresponding carbonyl compound [31,32]. The photolysis of arenesulfonylhydroxamates leads to a number of products that are consistent with S–N bond homolysis [33]. However, most of these processes required long irradiation times. Therefore, a PPG that is released efficiently and whose excitation does not lead to N–O bond homolysis should be capable of releasing HNO donors.

The aim of this study was to determine if mimics of HNO donors could be released by the *o*-nitrobenzyl (**2NBn**) PPG [24]. Benzohydroxamic acid (**1**) was selected to serve as model of sulfonylhydroxamate HNO donors because **1** was expected to be stable after release by **2NBn**. Since all HNO donors degrade to release HNO, a stable model (i.e. **1**) was used instead of attempting to directly release HNO donors, thus simplifying quantification of the products for this initial study. The **2NBn** PPG was selected since **2NBn** has been thoroughly investigated [34]. Also, the **2NBn** chromophore was expected to absorb light at higher wavelengths, which was expected to limit N–O bond homolysis reactions [35–37]. To examine this hypothesis, the photochemistry of nitro-substituted derivatives of benzyl benzohydroxamate (**Bn-1**) shown in Scheme 2 (i.e. 4-nitrobenzyl benzohydroxamate (**4NBn-1**), 2-nitrobenzyl benzohydroxamate (**2NBn-1**), and benzyl 4-nitrobenzohydroxamate (**Bn-4N-1**)) was examined.

2. Materials and methods

2.1. Computational methods

All calculations were performed with the Gaussian 09 suite of programs for electronic structure calculations [38]. The lowest energy conformation was determined from a number of rationally selected conformers that were optimized with HF/6-31G(d). These geometries were then further refined at the B3LYP/6-31G(d) level of theory, which were confirmed as minima by vibrational frequency calculations. Vertical excitation energies and oscillator strengths for singlet excited states were calculated using time-dependent DFT methods [39]. Structures and the difference between the ground and excited state density matrices were visualized using ChemCraft 1.6 [40].

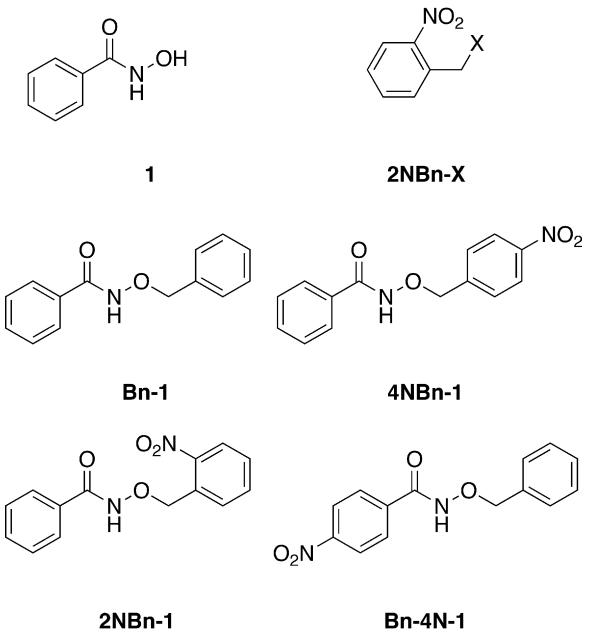

Scheme 2.

2.2. Materials

Commercial materials were obtained from Sigma–Aldrich or Fisher Scientific and used as provided unless specified otherwise. HPLC grade acetonitrile was dried by distilling over calcium hydride under inert atmosphere following procedure found in Armarego and Perrin [41]. Water was purified by a Milli-Q system. Benzyl benzohydroxamate (**Bn-1**) and 4-nitrobenzyl benzohydroxamate (**4NBn-1**) were prepared by the literature procedures [42,43].

2.2.1. Benzyl 4-nitrobenzohydroxamate (*Bn-4N-1*)

4-Nitrobenzoyl chloride (0.68 g, 4.10 mmol) and *O*-benzylhydroxylamine hydrochloride (0.65 g, 4.07 mmol) were dissolved in 60 mL of dry CH_2Cl_2 under nitrogen atmosphere. The reaction was allowed to stir for 15 min, and then 0.70 mL (8.65 mmol) of pyridine was added at 0 °C. The reaction mixture was allowed to proceed for 2 h at room temperature before being diluted with CH_2Cl_2 and washed three times with water. The organic layer was dried with anhydrous Na_2SO_4 and concentrated under reduced pressure. The resulting solid was recrystallized in toluene to give a colorless solid (0.49 g, 44.2%) with the same spectral profile as reported in the literature for the desired product [44]. Lit. m.p. = 166–167 °C, obs. m.p. = 167–168 °C.

2.2.2. 2-Nitrobenzyl benzohydroxamate (*2NBn-1*)

The desired compound was prepared following a modified procedure [45]. Benzohydroxamic acid (1.4 g, 10.0 mmol) was dissolved in 20 mL EtOH followed by the addition of 0.84 g (15.0 mmol) KOH dissolved in the minimum amount of water. In 50 mL of EtOH, 2-nitrobenzyl bromide (1.8 g, 8.3 mmol) was added dropwise. The solution was heated and allowed to reflux for 4.5 h and all of the 2-nitrobenzyl bromide had reacted. The mixture was then concentrated under reduced pressure and reconstituted with 80 mL of water. The product was extracted with chloroform (3× 60 mL), and the combined organic phases were washed with water (60 mL) and dried over anhydrous magnesium sulfate. The solvent was removed under reduced pressure, and the solid residue was then purified by column chromatography R_f = 0.39 (CH_2Cl_2/EtOAc 9:1) to yield a pale yellow solid. This solid was recrystallized in EtOH to yield 0.65 g (28.7%) of a colorless solid. Lit. m.p. = 121 [46] obs. m.p. = 119–120 °C; ^{1}H NMR ($CDCl_3$) δ = 8.76 (s br, 1H), 8.09 (d, J = 8.2 Hz, 1H), 7.95 (d, J = 7.6 Hz, 1H), 7.71 (m, 3H), 7.53 (m, 2H), 7.46 (m, 2H), 5.47 (s, 2H); IR (ATR) $\tilde{\nu}$ (cm^{-1}) = 3190, 3050, 2950, 1636, 1521, 1336.

2.3. Irradiations

Quantum yield measurements were carried out with a 75 W Xe arc lamp focused on a monochromator for wavelength selection. Slit widths allowed ±6 nm of linear dispersion from the set wavelength. Samples (4.8 mL) in a 1 cm quartz cell were placed in a permanently mounted cell holder such that all of the exiting light hit the sample without further focusing. For all direct quantum yield measurements, the concentration of the starting material was confirmed as sufficient to obtain a minimum absorbance of 2 at the selected wavelength, and the samples were irradiated

until approximately 15% conversion of the starting material was reached. Sensitized photoreactions were carried out at sufficient excess concentration of the photosensitizers to ensure at least 99% of the incident irradiation was absorbed by the sensitizer. Quenching experiments used 20 to 100-fold molar excess of the triplet quenchers. Prior to photolysis, most samples were sparged with argon for at least 15 min to remove oxygen. Other samples were carried out under freeze–pump–thaw conditions to rigorously exclude oxygen. Photolysis of azoxybenzene was used as an actinometer [47].

Due to the slow rates of conversion, percent yields of the observed products were determined from photolysis reactions carried out at 254 nm with a Luzchem LZC-4 photoreactor using low-pressure Hg lamps. Samples were held in standard fused-silica test tubes, and the starting concentrations (0.20 mM) were lowered to ease quantification of the loss of starting material. To ease quantification of the products, photoreactions were carried out to 30% conversion of the starting material. Thus, all percent yields are reported in respect to the theoretical maximum that could be obtained after 30% consumption of the starting material.

2.4. General methods

The concentrations of the starting materials and products at several time points during the photoreaction were quantified by HPLC analysis carried out with an Agilent 1100 Series instrument fitted with a diode array detector using a 150 mm/4.6 μm Eclipse XDB-C18 column. Products were identified by comparison to authentic samples and GC/MS analysis using a Shimadzu GCMS QP2010S using a DB-5 column for separations. The UV/Vis absorption spectra were obtained using a Shimadzu PharmaSpec UV-1700 system, and infrared spectra were obtained using a Perkin-Elmer Paragon FT-IR. NMR spectra were obtained using a Bruker DRX-400.

3. Results

A number of previous studies have shown the **2NBn** PPG to undergo an intramolecular hydrogen abstraction from the benzyl position generating an *aci*-nitro intermediate whose subsequent thermal chemistry releases the "caged" molecule [34,48–52]. Formation of the *aci*-nitro intermediate has been observed to form in less than 10 ps by picosecond pump–probe spectroscopy. For the photolysis of **2NBn-1**, the release of **1** was expected to dominate if the first excited singlet state (S_1) of **2NBn-1** favors hydrogen abstraction by the nitro group over N–O bond homolysis. For the parent **Bn-1,** photolysis led to predominantly N–O bond cleavage through a triplet Norrish Type II mechanism [31]. To better understand the excited states involved, the nature of the excited states of **Bn-1**, **2NBn-1**, **4NBn-1**, and **Bn-4N-1** were investigated by absorption spectroscopy and time-dependent density functional theory (TD-DFT) calculations.

The singlet ground (S_0) and triplet state (T_1) geometries of **Bn-1**, **2NBn-1**, **4NBn-1**, and **Bn-4N-1** were optimized at the B3LYP/6-31G(d) level of theory. Zero point energies were included when determining the energy of T_1 relative to S_0 at their equilibrium geometries. Vertical excitation energies and oscillator strengths for singlet excited states were calculated using time-dependent DFT methods [39], TD-B3LYP/6-31G(d). The vertical excitation energies (singlets), oscillator strengths, and T_1 energies are listed in Table 1.

The nature of the excited states was characterized through inspection of the difference of the single electron density matrix of the excited (P_{ex}) and ground states (P_0). The difference between the electronic density of S_1 and S_0 is depicted in Fig. 1 for **Bn-1** (a), **Bn-4N-1** (b), **2NBn-1** (c), and **4NBn-1** (e). Additionally, the difference densities of the S_2 state of **2NBn-1** (d) and S_3 of **4NBn-1** (f) are also illustrated. In Fig. 1, dark gray contours correspond to electron density accumulation in the excited state, and light gray corresponds to depletion from the ground state. For **Bn-1**, the character of the first excited state corresponds to a n, π^* state centered on the hydroxamate. Inspection of the difference density plot of **2NBn-1** and **4NBn-1** shows that the S_1 state is characterized by a (n, NO_2) → (π^*, NO_2) transition. The difference density of the S_1 state of **Bn-4N-1** reveals that electron density is transferred from the benzyl moiety to the nitro functional group, which suggests the S_1 of **Bn-4N-1** resembles a donor-bridge-acceptor intramolecular charge transfer (CT) state [53,54]. Visualization of the S_3 state of **4NBn-1** revealed transfer of electron density from the benzohydroxamate to the nitro group, which was similar to the donor-bridge-acceptor CT state observed for **Bn-4N-1**.

Potentially, release of **1** from **2NBn-1** would be decreased if pathways from higher energy excited states led to N–O homolysis. While internal conversion from higher singlet excited states (i.e. S_2–S_5) to S_1 is generally faster than other processes, poor overlap between the electronic or vibronic wave functions of two states results in slow internal conversion [55]. For **2NBn-1**, the S_2, S_3, and S_5 states were characterized by depletion of electron density from the benzohydroxamate moiety and an increase on the π^* orbital of the nitro group. Since the orbitals of the benzohydroxamate and the nitro groups were not conjugated, excitation into any of these states had the potential to allow processes not associated with S_1, which was expected to increase the possibility N–O bond homolysis.

Evidence indicating that irradiation of **2NBn-1** at longer wavelengths would lead to excitation of the **2NBn** chromophore was obtained from the UV/Vis spectra of **1**, **Bn-1**, **2NBn-1**, **4NBn-1**, and **Bn-4N-1** and 2-nitrotoluene. As shown in Fig. 2a, the molar extinction coefficient (ε) for **1** and 2-nitrotoluene dropped below 100 M^{-1} cm^{-1} at 300 nm and 368 nm, respectively. This indicated that 2-nitrotoluene had a lower energy S_1 state than **1**, and therefore, the S_1 state of **2NBn-1** was expected to be predominantly associated with the **2NBn** moiety. The absorption spectra for **2NBn-1** resembled a composite of the spectra obtained for **2NBn** and **1**, which suggested that the two observed absorption bands arose from localized chromophores.

For **Bn-4N-1** and **4NBn-1**, TD-DFT calculations found transitions with charge-transfer character had the largest oscillator strengths. To determine if the broad absorption bands centered near 265 nm for **Bn-4N-1** and **4NBn-1** arose from excitation into these CT states, the absorption spectra of **Bn-4N-1** and **4NBn-1** were obtained in chloroform, isopropanol, tetrahydrofuran, and acetonitrile. If the polarity of the ground state and excited state for the dominant absorption band were different, a positive solvatochromic shift would be expected. However, only a small bathochromic shift was observed for both compounds (**Bn-4N-1**; λ_{max} $CHCl_3$ (262.9 nm) ACN (264.1 nm), **4NBn-1**; λ_{max} $CHCl_3$ (266.0 nm) ACN (267.0 nm)). This small positive solvatochromic shift indicated that for both **Bn-4N-1** and **4NBn-1** the polarity of the ground state and excited state were similar.

Since all HNO donors spontaneously decompose in certain conditions, benzohydroxamic acid (**1**) was selected as a stable model of a HNO donor. By investigating the photochemistry of benzohydroxamates and the photoactivated release of **1** from **2NBn-1**, it was expected that insights valuable to the use of this PPG to release HNO donors would be gained. The parent benzyl benzohydroxamate (**Bn-1**) has been investigated previously, and it was concluded that **Bn-1** undergoes a triplet Type II photoelimination to yield benzamide (**2**) and benzaldehyde (**3**) [31]. In similar conditions and at lower concentrations, we found that photolysis of **Bn-1** yields mainly **2** and **3** as the primary photoproducts, and these results are summarized in Fig. 3. In the original work, it was stated that the carbonyl products were generally not observed, and an unknown by-product was often present. In our photolysis of **Bn-1**, benzyl alcohol and benzoic acid were confirmed as products

Table 1
Computationally predicted electronic configurations, excitation energies, and oscillator strength of selected excited states.

State	Electron configuration[a]	Vert. ex. E[b]	f[c]	$E(T_1 - S_0)$[d]
Bn-1				
S_1	n(CO), π^*(CO)	102.3 (279.3 nm)	0.0019	
S_2	n(CO), π^*(CO)	114.2 (250.2 nm)	0.0282	
T_1	n(CO), π^*(CO, aryl)			74.1
2NBn-1				
S_1	$n(NO_2)$, $\pi^*(NO_2)$	86.9 (329.1 nm)	0.0116	
S_2	n(CO), $\pi^*(NO_2)$	88.6 (322.58 nm)	0.0018	
S_3	n(CO), $\pi^*(NO_2)$	97.3 (293.81 nm)	0.0009	
S_4	$n(NO_2)$, $\pi^*(NO_2)$	98.9 (289.00 nm)	0.0008	
S_5	Tr(aryl), $\pi^*(NO_2)$	102.1 (279.96 nm)	0.0254	
T_1	n(CO), $\pi^*(NO_2$, aryl)			52.7
4NBn-1				
S_1	$n(NO_2)$, $\pi^*(NO_2)$	86.8 (329.6 nm)	0.0000	
S_2	n(CO), $\pi^*(NO_2)$	91.5 (312.4 nm)	0.0001	
S_3	CT (aryl, NO_2)	95.4 (299.81 nm)	0.0138	
T_1	n(CO), π^*(CO, aryl)			77.0
Bn-4N-1				
S_1	CT (aryl, NO_2)	82.2 (347.8 nm)	0.0056	
S_2	CT (aryl, NO_2)	85.2 (335.7 nm)	0.0008	
T_1	π(aryl), $\pi^*(NO_2$, aryl)			63.5

[a] Singlet characterized by the difference between the excited and ground state electron density matrix. Triplet characterized by examining singly occupied molecular orbitals.
[b] Vertical excitation energy (kcal mol^{-1}).
[c] Oscillator strength.
[d] kcal mol^{-1}, includes ZPE correction.

by chromatographic comparison to authentic samples. Typically, benzyl alcohol and benzoic acid were minor products; however, considerable variation in their product yields was observed. It was also confirmed that photosensitization by irradiating **Bn-1** in an excess of benzophenone at 350 nm led to the same products. Thus, the previously postulated Type II photoelimination from the triplet state was verified.

While photolysis of **2NBn-1** was expected to release **1**, it was unclear if the addition of the nitro functional group would activate other side reactions, and thus, the effect of nitro substitution on the photochemistry of **Bn-1** was examined. Unlike **Bn-1**, the lowest excited singlet of **Bn-4N-1** was predicted by TD-DFT to be a charge transfer state (essentially a zwitterionic diradical) [54]. The photolysis of **Bn-4N-1** in wet acetonitrile led to **3**, 4-nitrobenzamide (**4**) and 4-nitrobenzoic acid (**5**) with a mass balance near 75%. A similar result was obtained when the solvent was dried; however, the mass balance dropped to 40%. The products and quantum yields for these products are shown in Table 2. To ensure the observed products did not arise from a thermal reaction, control solutions were kept at 35 °C for 4 days in the dark. No decomposition of **Bn-4N-1** or the appearance of products was detected in these control experiments.

Regardless of the conditions, the quantum yields for these reactions were very low (less than 0.005). The ratio of **4:5** was 1:4, respectively, and their combined yield roughly correlated with the yield of **3**. However, when the photolysis was run in dry acetonitrile, the ratio of **4:5** decreased to 1:1. It was also observed that performing the photolysis under ambient atmosphere had no effect on the observed quantum or product yields. Additionally, rigorous exclusion of oxygen by five freeze–pump–thaw cycles had no effect on the product ratio obtained in a 2% water acetonitrile mixture upon photolysis at 294 nm. Thus, it was believed that a significant portion of **5** arose from the hydrolysis of excited **Bn-4N-1** and not oxidation by a trace amount of advantageous oxygen.

The TD-DFT predicted electronic configuration of S_1 for both **2NBn-1** and **4NBn-1** was $n(NO_2)$, $\pi^*(NO_2)$; however, only for **2NBn-1** was the location of nitro group amenable to abstraction of the benzyl hydrogen leading to the release of **1**. Thus, investigation of the photochemistry of **4NBn-1** was expected to provide insight into side reactions with the potential to compete with the release of the **2NBn**. Photolysis of **4NBn-1** in wet

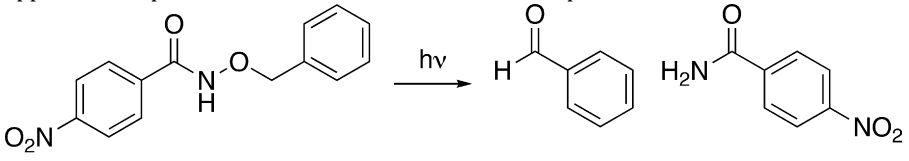

Bn-4N-1 **3** **4**

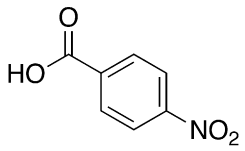

5

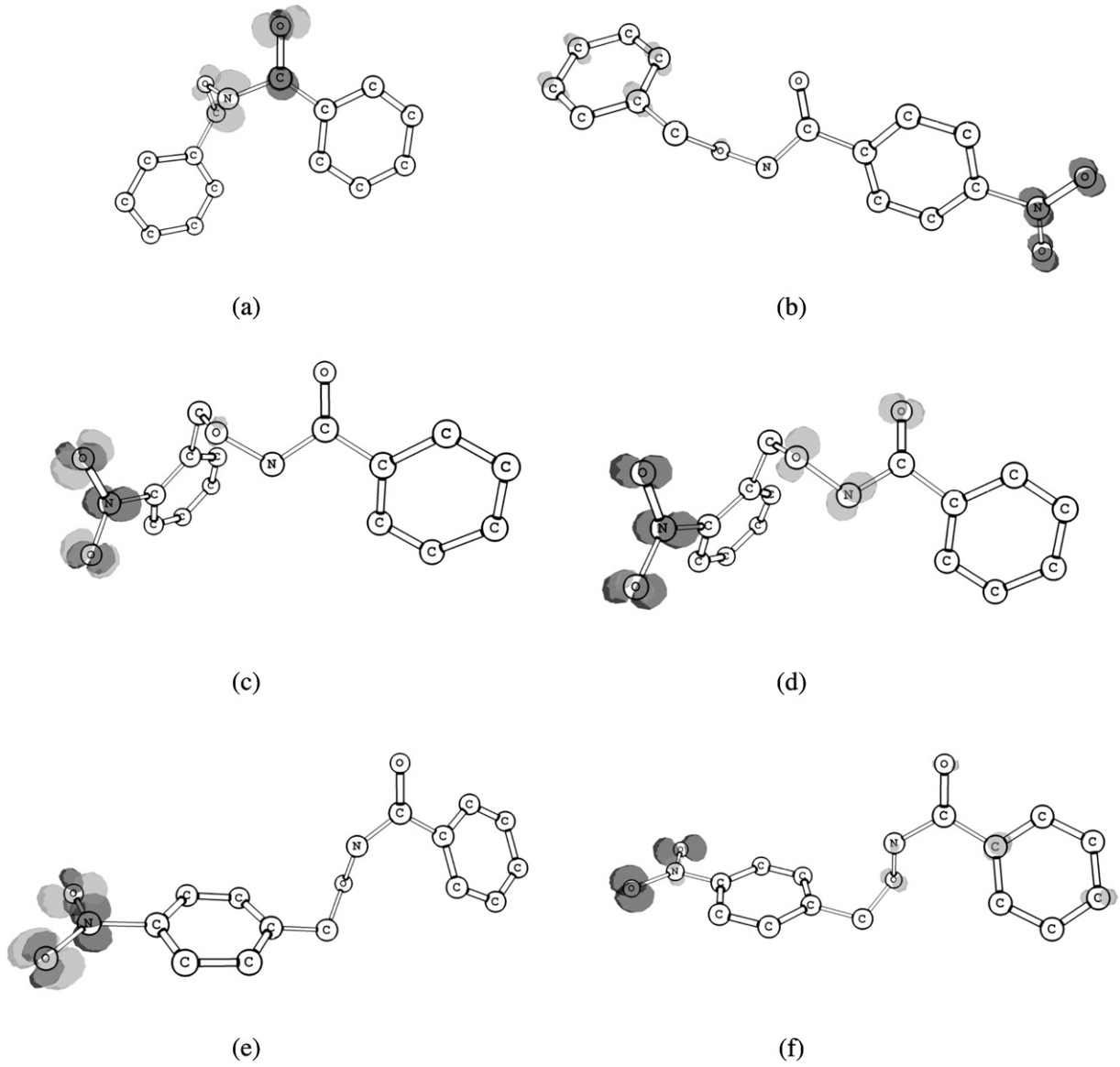

Fig. 1. TD-B3LYP/6-31G(d) excited-state difference density plots (excited-state less the ground-state density). A dark gray shading indicates an area where electron density is accumulated in the excited-state, and light gray shading represents an area from where the electron density is depleted from S_0. (a) S_1 **Bn-1**, (b) S_1 **Bn-4N-1**, (c) S_1 **2NBn-1**, (d) S_2 **2NBn-1**, (e) S_1 **4NBn-1**, and (f) S_3 **4NBn-1**. The surfaces were determined with a ±0.023 a.u. isocountour value, and hydrogen atoms were not shown to improve figure clarity.

Table 2
Product and quantum yields of the photolysis of benzyl 4-nitrobenzohydroxamate (**Bn-4N-1**).

Entry	Solvent	λ (nm)	**3**	**4**	**5**
1	MeCN/2%H_2O	254	0.0030 ± 7[a] (84 ± 15)[b]	0.00057 ± 14[a] (17 ± 3)[b]	0.0023 ± 12[a] (61 ± 13)[b]
2	MeCN/2%H_2O	294	0.00063 ± 29[a] (67 ± 2)[b]	0.00023 ± 3[a] (14 ± 1)[b]	0.00089 ± 42[a] (66 ± 17)[b]
3	MeCN	254	(38 ± 9)[b]	(20 ± 11)[b]	(24 ± 2)[b]

[a] Φ ±95% confidence interval of last digits.
[b] % Yield relative to loss of **Bn-4N-1** ±95% confidence interval of last digit(s). % Yields determined at 30% conversion of **Bn-4N-1**.

acetonitrile produced a complex product mixture, and the dominant products in this mixture were 4-nitrobenzaldehyde (**6**), benzamide (**7**), benzoic acid (**8**), and 4-nitrobenzyl alcohol (**9**). Product percent yields of these products are listed in Table 3. Similar to **Bn-4N-1**, the quantum yields for the formation of these products were less than 0.006 at 294 nm. Quantum yields at 254 nm could not be accurately measured due to the slow rate of photoreaction.

Table 3
Product and quantum yields of the photolysis of 4-nitrobenzyl benzohydroxamate (**4NBn-1**).

Entry	λ (nm)	Solvent	Additive/technique	**6**	**7**	**8**	**9**
1	254	MeCN/2%H_2O		(52 ± 24)[a]	(54 ± 10)[a]	(6.0 ± 4.4)[a]	(3.0 ± 1.8)[a]
2	254	MeCN		(50 ± 15)[a]	(83 ± 17)[a]	(6.7 ± 0.4)[a]	(13±2)[a]
3	254	MeCN/2%H_2O	O_2[b]	(74 ± 28)[a]	(40 ± 15)[a]	(15 ± 3)[a]	(3.0 ± 3.9)[a]
4	294	MeCN/2%H_2O		0.0041 ± 16[c]	0.0012 ± 5[c]	0.0022 ± 14[c]	0.00038 ± 14[c]
5	294	MeCN		0.0057 ± 8[c]	0.0012 ± 2[c]	0.0013 ± 6[c]	0.00059 ± 18[c]
6	294	MeCN/2%H_2O	FPT[d]	0.0011 ± 4[c]	0.0012 ± 3[c]	n.d.[e]	0.00017 ± 8[c]
7	294	MeCN/2%H_2O	Diene[f]	–[g]	0.0018 ± 5[c]	0.00033 ± 14[c]	n.d.[e]
8	360	MeCN/2%H_2O	Ph_2CO[h]	–[g]	(13 ± 16)[a]	(75 ± 9)[a]	(18 ± 6)[a]

[a] % Yield relative to loss of **4NBn-1** ±95% confidence interval of last digit(s). % Yields determined at 30% conversion of **4NBn-1**.
[b] Sparged with O_2 gas for 20 min before photolysis.
[c] Φ ±95% confidence interval of last digit(s).
[d] Freeze–pump–thaw cycles.
[e] Not detected.
[f] The addition of 2,4-dimethyl-1,3-pentadiene (80 mM).
[g] Could not be determined.
[h] Benzophenone (80 mM) sensitized photoreaction.

Table 4
Product and quantum yields of the photolysis of 2-nitrobenzyl benzohydroxamate (**2NBn-1**).

Entry	Solvent	λ (nm)	**1**	**7**	**10**
1	MeCN/2%H_2O	254	0.064 ± 12[a] (45 ± 7)[b]	0.033 ± 7[a] (37 ± 4)[b]	0.042 ± 9[a] (40 ± 4)[b]
2	MeCN/2%H_2O	294	0.14 ± 1[a]	0.062 ± 4[a]	0.059 ± 25[a]
3	MeCN/2%H_2O	340	0.18 ± 4[a]	0.053 ± 11[a]	0.029 ± 8[a]

[a] Φ ±95% confidence interval of last digit(s).
[b] % Yield relative to loss of **2NBn-1** ±95% confidence interval of last digit(s). % Yields determined at 30% conversion of **2NBn-1**.

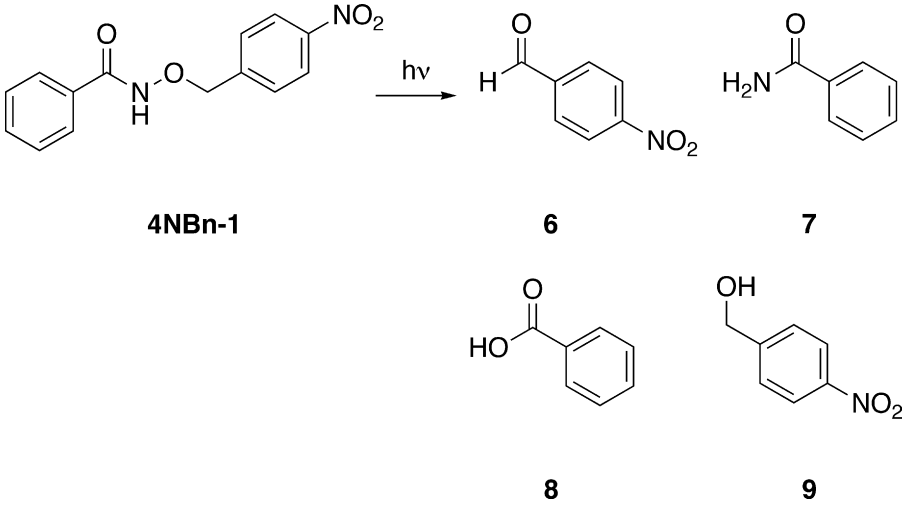

For **Bn-4N-1**, the formation of the benzoic acid product appeared to arise from hydrolysis of an excited state. However, unlike **Bn-4N-1**, no change in the product or quantum yields of benzoic acid was observed when the photolysis of **4NBn-1** was carried out in dry acetonitrile. Therefore, the effect of oxygen, triplet sensitizers, and triplet quenchers was examined. Rigorous exclusion of O_2 by five freeze–pump–thaw cycles prevented the formation of benzoic acid (**8**) and had little effect on the quantum yields of **6**, **7**, and **9**. Conversely, sparging the solution with O_2 prior to irradiation resulted in a 3-fold increase in the yield of **8**. The addition of a 20-fold excess of the triplet quencher 2,4-dimethylpentadiene (80 mM) also resulted in a 10-fold reduction in the quantum yield of benzoic acid while having a minimal effect on the quantum yields of **7**, and **9**. The quantum yield of **6** could not be measured due to a co-eluting peak in the chromatography. Irradiation of **4NBn-1** at 360 nm in excess concentrations (80 mM) of the photosensitizer benzophenone resulted in benzoic acid being the major product. Again, the yield of **6** could not be measured due to a co-eluting peak.

The stated aim of this work is to use the **2NBn** PPG to photochemically release **1** as a way to gain insight into the release of HNO donors. One concern to the yield of **1** was the photosensitive N–O bond of benzohydroxamates. The UV/Vis spectrum of **2NBn-1** closely resembled a superposition of **1** and 2-nitrotoluene, which indicated that transitions associated with the two absorption bands were localized on either the **1** or the **2NBn** chromophores. Since the λ_{max} of **1** was 225 nm, the first absorption band centered at 225 nm for **2NBn-1** was assigned to the benzohydroxamate chromophore, and shoulder beginning

at 260 nm and extending out to 370 nm to the **2NBn** chromophore. It was thought possible that since absorption appeared localized that wavelength-dependent photochemistry might be observed. Thus, the irradiation was carried out at three different wavelengths: 254, 294, and 340 nm. These wavelengths were selected since they covered the range of the UV absorption by **2NBn-1** and corresponded with the reported quantum yields for the azoxybenzene actinometer. As seen in Table 4, the major product at all wavelengths was **1**, and quantum yields for the formation of

1 increased at longer wavelengths. The minor products **7** and 2-nitrobenzaldehyde (**10**) were observed at all wavelengths, and the quantum yields for the formation of **7** and **10** were constant, within experimental error, at the three wavelengths examined. The release of the **2NBn** PPG typically yields a 2-nitrosobenzaldehyde remnant, which is known to undergo thermal or photoinduced decomposition and was not detected in this study [34].

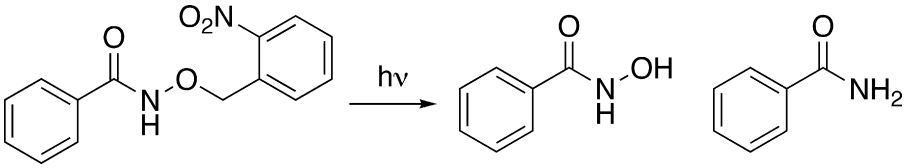

2NBn-1 **1** **7**

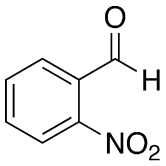

10

While the above result clearly indicates that release of **1** by the **2NBn** PPG was the dominant process, it was unclear how **7** and **10** were being generated. To determine if these minor products were the result of a Type II photoelimination as observed for **Bn-1**, the effects of common triplet quenchers and photosensitizers were examined. As seen in Table 5, the addition of 1,3-cyclohexadiene and *p*-terphenyl led to slightly decreased quantum yields of **1**. Additionally, oxygen quenched the formation of **1**. The quantum yields of **7** and **10** were largely unaffected or even slightly increased upon the addition of the triplet quenchers. The T_1 energy predicted by B3LYP/6-31G(d) suggested energy transfer for photosensitizers with triplet energies above 53 kcal mol^{-1} should be thermodynamically favorable. However, no reaction was observed with photosensitizers with triplet energies under 60 kcal mol^{-1}. Only benzophenone, which has a triplet energy of 69 kcal mol^{-1} [56], was able to photosensitize the formation of **1**, **7** and **10**.

4. Discussion

In order to develop photoactivated HNO precursors, the overall goal of these studies was to examine the effect of nitro substitution on the photochemistry of **Bn-1**. Homolysis of the N–O bond was expected to be the main challenge to the release of the HNO donor mimic **1**, and thus, the effect of nitro substitution at different positions on the parent **Bn-1** on N–O bond homolysis was examined.

The nature of the S_1 state was found to have an effect on the observed photochemistry. Results from TD-DFT calculations indicated that irradiation of **Bn-4N-1** would generate a CT state. Since the S_1 state of **Bn-1** was n, π^*, it was expected that the photochemistry of **Bn-4N-1** would be different than the parent. Unlike **Bn-1**, which only produced benzoic acid in trace amounts, photolysis of **Bn-4N-1** in wet acetonitrile led to a significant amount of 4-nitrobenzoic acid (**5**) as seen in entries 1 and 2 of Table 2. Additionally, removal of water (Table 2, entry 3) led to a decrease in the amount of **5** compared to the other nitro-containing product (**4**), and thus, the formation of **5** appeared to arise from the hydrolysis of photoexcited **Bn-4N-1**. The enhancement of solvolysis by nitro substitution had also been previously reported for phenyl 4-nitrobenzoate, where irradiation in ethanol led to transesterification rather than the expected photo-Fries rearrangement [57].

Unlike **Bn-4N-1**, the lowest energy singlet excited state for **4NBn-1** was $n(NO_2)$, $\pi^*(NO_2)$ rather than a CT state. Since the S_1 electronic configuration of **2NBn-1** was also $n(NO_2)$, $\pi^*(NO_2)$, the photochemistry of **4NBn-1** was expected to resemble **2NBn-1** more than **Bn-4N-1** if internal conversion to S_1 was efficient. Additionally, since the position of the nitro group is critical for the photoinduced release of **2NBn**, the photoreactions of **4NBn-1** were expected to provide insights into processes that could be competitive with the release of **1** from **2NBn-1**. Therefore, the low quantum yields for the photoreactions of **4NBn-1** in Table 3 were encouraging for the potential of **2NBn-1** to release **1**.

It was considered that benzoic acid could potentially arise from the hydrolysis of the S_3 CT state of **4NBn-1**, as with **Bn-4N-1**. However, when **4NBn-1** was photolyzed in dry acetonitrile, no change in the amount of benzoic acid (**8**) was observed as shown in Table 3 (entries 1 and 2). While water content had no effect, exposure to O_2 led to higher product yields of benzoic acid (entry 3). Likewise, rigorous exclusion of oxygen prevented the formation of benzoic acid (entries 4 and 6). The effect of O_2 can also be used to explain the discrepancy between the reported product yields at 254 nm and the quantum yields at 294 nm (entries 1 and 4). For the photoreactions used to determine product percent yields, a greater photon flux generated by low pressure mercury bulbs was used, and thus, the photoreactions were complete in less than hour. Due to the comparatively lower photon flux generated by the Xe arc lamp, quantum yield measurements were preformed over the course of 12 h, and multiple time-points were analyzed from the same sample. Thus, the quantum yield measurements were at higher risk for contamination by O_2.

Since triplet sensitization by benzophenone dramatically increased the yield of benzoic acid (Table 3, entry 8), it was concluded that benzoic acid arose primarily from a T_1 reaction with advantageous oxygen in solution. This hypothesis was supported by the 4-fold decrease in the quantum yield of benzoic acid when a diene triplet quencher was added to the solution as shown in Table 3 entry 7. The percent yields of the other major products **6** and **7** were not affected by water, O_2, or dienes, and thus, the formation of **6** and **7** was proposed to arise from the S_1 state. It is possible that **6** and **7** were the result of an N–O bond homolysis followed by disproportionation as shown in Scheme 3. The minor alcohol product **9** was likely the result of the nascent alkoxy radical, arising from

Table 5
Quantum yields for 2-nitrobenzyl benzohydroxamate (**2NBn-1**) with various triplet photosensitizers and quenchers.

Entry	Additives	T_1[a]	λ (nm)	**1**	**7**	**10**
1	Oxygen	23	340	0.047 ± 4[b]	0.10 ± 1	0.062 ± 3
2	1,3-Cyclohexadiene	53	340	0.11 ± 3	0.041 ± 10	0.015 ± 4
3	*p*-Terphenyl	58	340	0.13 ± 2	0.099 ± 32	0.062 ± 18
4	Acridine	45	340	n.d.[c]	n.d.	n.d.
5	9-Fluorenone	50	360	n.d.	n.d.	n.d.
6	2-Acetonaphthalene	59	360	n.d.	n.d.	n.d.
7	Benzophenone	69	360	0.063 ± 33	0.058 ± 30	0.024 ± 17

[a] Triplet energies taken from Ref. [56].
[b] Φ ±95% confidence interval of last digit(s).
[c] Not detected.

N–O bond homolysis, abstracting a hydrogen atom from a solvent molecule.

Since the absorption band centered at 225 nm of **2NBn-1** was believed to be localized on the benzohydroxamate chromophore, it was a concern that irradiation at shorter wavelengths would increase the percent yields of products associated with N–O bond cleavage. The **2NBn** chromophore was expected to absorb light at higher wavelengths than the benzohydroxamate moiety of **2NBn-1**. The use of monochromatic irradiation at longer wavelengths has been used to selectively activate one photoreactive center over another center on the same molecule [35,37]. Thus, it was expected

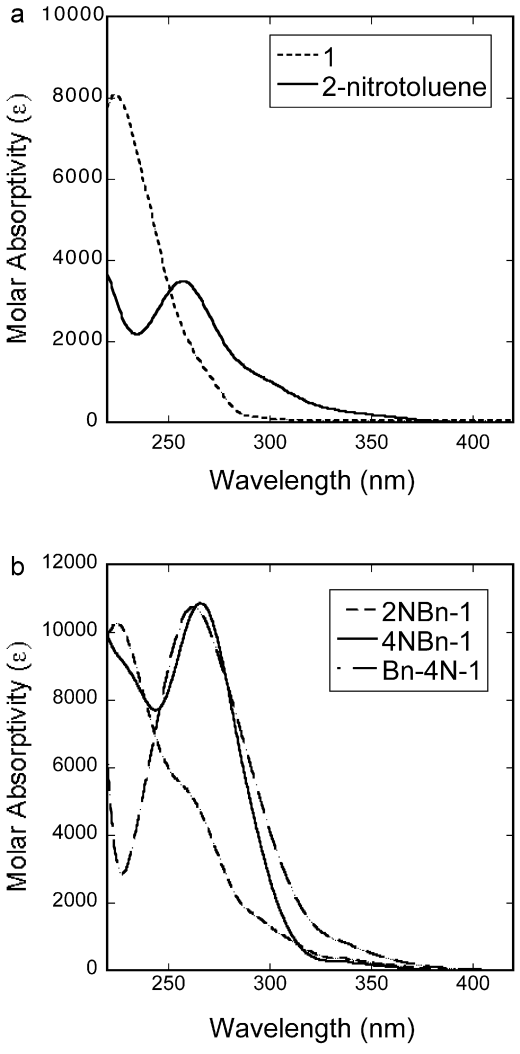

Fig. 2. UV/Vis spectra in acetonitrile. (a) Solid line (2-nitrotoluene), short dash line (1). (b) Short dash line (2NBn-1), solid line (4NBn-1), long dash line **(Bn-4N-1)**.

that irradiation at longer wavelengths would favor the release of the **2NBn** PPG by the mechanism shown in Scheme 4. Indeed, an increase in the quantum yield for **1** was observed as the wavelength of irradiation was increased as shown in Table 4. This indicated that localized absorption by the **2NBn** chromophore favored abstraction of the benzyl hydrogen leading to the *aci*-nitro intermediate (**I**) and the subsequent steps leading to the release of **1** [34].

The B3LYP/6-31G(d) T_1 energy of **2NBn-1** was 52.7 kcal mol^{-1}, however, only irradiation of benzophenone (T_1 = 69 kcal mol^{-1} [56]) and not 2-acetonaphthone (T_1 = 59 kcal mol^{-1} [56]) was able to induce the release of **1** as shown in Table 5 entries 4–7. This suggested that the actual triplet energy of **2NBn-1** was between 60 and 70 kcal mol^{-1} and the release of **1** can occur through the triplet state. Supporting this assertion was the observed quenching of the formation of **1** by the addition the triplet quenchers of *p*-terphenyl and 1,3-cyclohexadiene (entries 2 and 3). Picosecond-pump probe experiments have been used to suggest that the triplet state of **2NBn** can abstract the benzylic hydrogen leading to a triplet biradical that converts to **I** [49]. However, the quenching was modest, which indicates that most of the release of **1** upon direct photolysis of **2NBn-1** occurs through S_1.

As shown in Scheme 5, three different processes were considered as possible pathways to the minor products **7** and **10**. The first was abstraction of the benzylic hydrogen by the carbonyl initiating a Type II photoelimination (Scheme 5a). The second was N–O bond homolysis followed by disproportionation (Scheme 5b). Finally, it was considered possible that the minor products **7** and **10** were generated from an alternative degradation of the *aci*-nitro intermediate (**I**) (Scheme 5c).

Since both pathways (a) and (b) shown in Scheme 5 were most likely to arise from excitation of the benzohydroxamate chromophore, the quantum yields of **7** and **10** were expected to decrease at longer wavelengths as the absorption by the **2NBn** moiety increased. However, irradiation at 340 nm still generated **7** and **10** in significant amounts (Table 4, entry 3). A few different possibilities were considered to explain this observation at longer wavelengths. Since benzophenone triplet sensitization yielded significant amounts of **7** and **10** compared to **1**, it was considered that the formation of **7** and **10** arose from triplet state after intersystem crossing. However, triplet quenchers had no effect or even increased the observed quantum yields for **7** and **10** (Table 5, entries 1–3), and thus, it was concluded that the formation of **7** and **10** predominantly proceeds through a singlet excited state under direct photolysis conditions. Only a very small difference in energy of S_1 and S_2 was predicted by TD-DFT calculation, and thus, S_2 should be accessible at longer wavelengths. The S_2 state of **2NBn-1** was characterized by TD-DFT as n(CO), π^*(NO_2), which could potentially undergo a Type II mechanism (Scheme 5a). However, for **7** and **10** to arise from S_2, slow relaxation from S_2 to S_1 would be required, which was considered unlikely. The much lower quantum yields of **6** and **7** for **4NBn-1** suggest the minor products **7** and **10** were due to a photochemical processes specific to **2NBn-1**, which argues

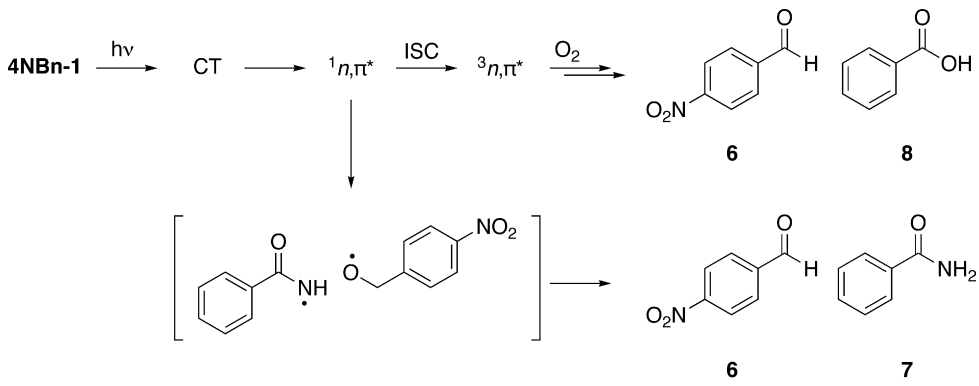

Scheme 3.

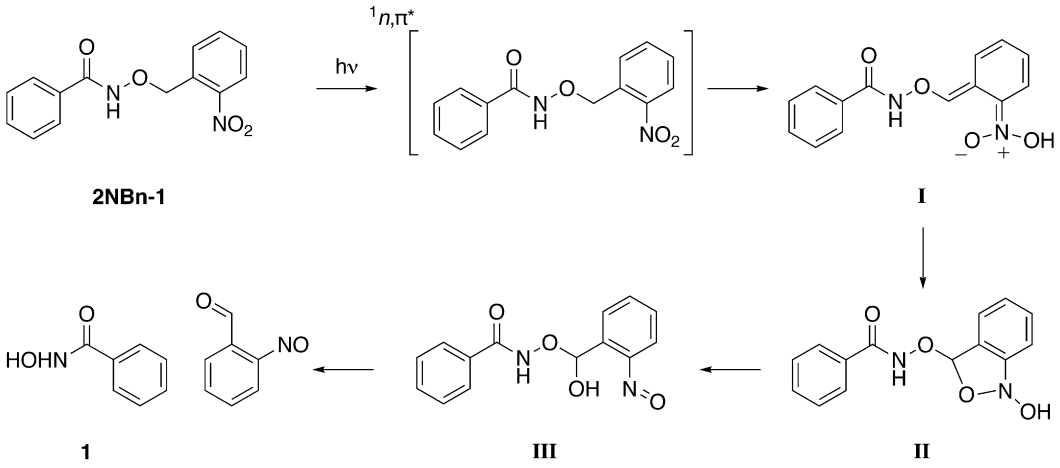

Scheme 4.

against the N–O bond homolysis mechanism (Scheme 5b). Thus, it was thought most likely that the minor products **7** and **10** arose from an alternative degradation of **I** (Scheme 5c).

If **1**, **7**, and **10** arose solely from the decomposition of **I**, it would be expected that the ratio of the products would remain constant over the wavelengths examined. However, the amount of **1** compared to **7** and **10** decreases at shorter wavelengths. This indicates that another process leading to **7** and **10** becomes operative at shorter wavelengths. It is possible that excess vibrational energy generated with the higher energy photons leads to N–O bond homolysis (Scheme 5b). Alternatively, excitation into a π, π^*, such as S_5 which has a high oscillator strength, eases intersystem crossing into n, π^* triplet states [58]. This assertion was consistent with the similar product ratio observed for 254 nm directirradiation (Table 4, entry 1) and benzophenone photosensitization at 360 nm (Table 5, entry 7).

For the benzophenone-sensitized photoreaction, analysis of the B3LYP/6-31G(d) molecular orbitals of the triplet state (T_1) of **2NBn-1** found that the two SOMO's were centralized on the carbonyl oxygen and the nitro substituent. While abstraction of the benzylic hydrogen by the nitro substituent would eventually lead to **I** and eventually **1**, abstraction by the carbonyl would lead to a Type II elimination (Scheme 5a) and the minor products **7** and

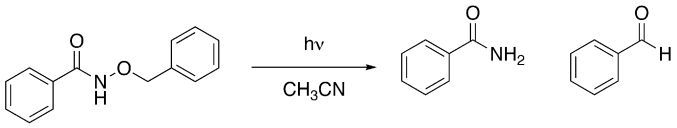

		2	3
		% yield[a]	% yield[a]
0.1 M	254 nm	74 ± 21[b]	35 ± 14[b]
0.001 M	254 nm	85 ± 8[b]	57 ± 7[b]

Fig. 3. Yields of products upon photolysis of benzyl benzohydroxamate (Bn-1). [a]Percent yields relative to loss of **Bn-1** at 30% conversion, [b]uncertainty reported as 95% confidence interval.

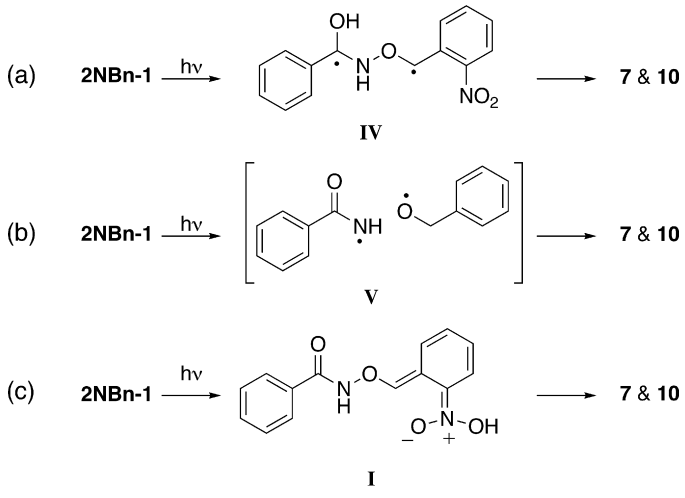

Scheme 5.

10. Thus, product yields for the benzophenone sensitization may reflect competition for the benzylic hydrogen between the carbonyl (Scheme 5a) and the nitro (Scheme 5c) functional groups.

5. Conclusions

The stated aim of this work was to determine if selective excitation of the **2NBn** chromophore within **2NBn-1** would result in increased release of **1**. Quantum yields for the formation of **1** increased at longer wavelengths and the percent yields of the minor products decreased, which supported the proposed hypothesis. The totality of these results also suggested that all of the products formed during direct photolysis of **2NBn-1** can be formed from either the S_1 or the T_1 state. Given the wavelength-dependent quantum yields for **1**, the relatively constant quantum yields for the minor products **7** and **10** over several wavelengths were taken as an indication that two different processes were responsible for the formation of **7** and **10**. At longer wavelengths, it was suspected that an alternative decomposition of **I** gave rise to these minor products. Irradiation at higher energies was thought to allow easier access to the triplet manifold through a π, π^* singlet. Photosensitization indicated that equal amounts of **1** and **7** were formed from T_1. The position of the nitro substituent also influenced the observed photochemistry. When the lowest energy excited state had charge transfer character, hydrolysis became possible. Positioning of the nitro substituent to disfavor the hydrogen abstraction dramatically decreased the quantum yields for the loss of the starting materials, and thus, the addition of a nitro substituent was not expected to increase the amount of N–O bond homolysis.

References

[1] W. Flores-Santana, C. Switzer, L.A. Ridnour, D. Basudhar, D. Mancardi, S. Donzelli, D.D. Thomas, K.M. Miranda, J.M. Fukuto, D.A. Wink, Arch. Pharm. Res. 32 (2009) 1139–1153.
[2] N. Paolocci, M. Jackson, B. Lopez, K. Miranda, C. Tocchetti, D. Wink, A. Hobbs, J. Fukuto, Pharmacol. Therapeut. 113 (2007) 442–458.
[3] J.M. Fukuto, M.D. Bartberger, A.S. Dutton, N. Paolocci, D.A. Wink, K.N. Houk, Chem. Res. Toxicol. 18 (2005) 790–801.
[4] D.A. Wink, K.M. Miranda, T. Katori, D. Mancardi, D.D. Thomas, L. Ridnour, M.G. Espey, M. Feelisch, C.A. Colton, J.M. Fukuto, P. Pagliaro, D.A. Kass, N. Paolocci, Am. J. Physiol. Heart Circ. Physiol. 285 (2003) H2264–H2276.
[5] K.M. Miranda, N. Paolocci, T. Katori, D.D. Thomas, E. Ford, M.D. Bartberger, M.G. Espey, D.A. Kass, M. Feelisch, J.M. Fukuto, D.A. Wink, Proc. Natl. Acad. Sci. U. S. A. 100 (2003) 9196–9201.
[6] E.G. DeMaster, B. Redfern, H.T. Nagasawa, Biochem. Pharmacol. 55 (1998) 2007–2015.
[7] H.T. Nagasawa, E.G. DeMaster, B. Redfern, F.N. Shirota, D.J. Goon, J. Med. Chem. 33 (1990) 3120–3122.
[8] N. Paolocci, T. Katori, H. Champion, M. St John, K. Miranda, J. Fukuto, D. Wink, D. Kass, Proc. Natl. Acad. Sci. U. S. A. 100 (2003) 5537–5542.
[9] P. Pagliaro, D. Mancardi, R. Rastaldo, C. Penna, D. Gattullo, K.M. Miranda, M. Feelisch, D.A. Wink, D.A. Kass, N. Paolocci, Free Radic. Biol. Med. 34 (2003) 33–43.
[10] C.G. Tocchetti, W. Wang, J.P. Froehlich, S. Huke, M.A. Aon, G.M. Wilson, G. Di Benedetto, B. O'Rourke, W.D. Gao, D.A. Wink, J.P. Toscano, M. Zaccolo, D.M. Bers, H.H. Valdivia, H. Cheng, D.A. Kass, N. Paolocci, Circ. Res. 100 (2007) 96–104.
[11] J.M. Fukuto, K. Chiang, R. Hszieh, P. Wong, G. Chaudhuri, J. Pharmacol. Exp. Ther. 263 (1992) 546–551.
[12] E. Bermejo, D.A. Sáenz, F. Alberto, R.E. Rosenstein, S.E. Bari, M.A. Lazzari, Thromb. Haemost. 94 (2005) 578–584.
[13] A. Ellis, C.G. Li, M.J. Rand, Br. J. Pharmacol. 129 (2000) 315–322.
[14] W. Kim, Y. Choi, P. Rayudu, P. Das, W. Asaad, D. Arnelle, J. Stamler, S. Lipton, Neuron 24 (1999) 461–469.
[15] B. Lopez, D. Wink, J. Fukuto, Arch. Biochem. Biophys. 465 (2007) 430–436.
[16] M. Doyle, S. Mahapatro, R. Broene, J. Guy, J. Am. Chem. Soc. 110 (1988) 593–599.
[17] S. Maraj, S. Khan, X. Cui, R. Cammack, C. Joannou, M. Hughes, Analyst 120 (1995) 699–703.
[18] H. Ohshima, I. Gilibert, F. Bianchini, Free Radic. Biol. Med. 26 (1999) 1305–1313.
[19] F. Kohout, F. Lampe, J. Am. Chem. Soc. 87 (1965) 5795–5796.
[20] V. Shafirovich, S.V. Lymar, Proc. Natl. Acad. Sci. U. S. A. 99 (2002) 7340–7345.
[21] K.M. Miranda, H.T. Nagasawa, J. Toscano, Curr. Top. Med. Chem. 5 (2005) 649–664.
[22] Y. Adachi, H. Nakagawa, K. Matsuo, T. Suzuki, N. Miyata, Chem. Commun. (2008) 5149–5151.
[23] A.D. Cohen, B.B. Zeng, S.B. King, J.P. Toscano, J. Am. Chem. Soc. 125 (2003) 1444–1445.
[24] G. Mayer, A. Heckel, Angew. Chem. Int. Ed. 45 (2006) 4900–4921.
[25] R.S. Givens, P.G. Conrad, A.L. Yousef, J. Leel, CRC Handbook of Organic Photochemistry and Photobiology, second ed., CRC Press, Boca Raton, 2004 (Chapter 69).
[26] C. Walling, A.N. Naglieri, J. Am. Chem. Soc. 82 (1960) 1820–1825.
[27] T. Sakurai, S. Yamada, H. Inoue, Chem. Lett. (1983) 4975–4978.
[28] T. Sakurai, H. Yamamoto, S. Yamada, H. Inoue, Bull. Chem. Soc. Jpn. 58 (1985) 1174–1181.
[29] B. Hosangadi, P. Chhaya, M. Nimbalkar, N. Patel, Tetrahedron 43 (1987) 5375–5380.
[30] E. Lipczynska-Kochany, Chem. Rev. 91 (1991) 477–491.
[31] J.E. Johnson, M. Arfan, R. Hodzi, L.R. Caswell, S. Rasmussen, Photochem. Photobiol. 51 (1990) 139–144.
[32] R. White, K. Oppliger, J. Johnson, J. Photochem. Photobiol. A 101 (1996) 197–200.
[33] M.M. Aly, A.M. Fahmy, F.F. Abdellatif, M.Z.A. Badr, Bull. Pol. Acad. Sci., Chem. 35 (1987) 47–52.
[34] Y. Il'ichev, M. Schworer, J. Wirz, J. Am. Chem. Soc. 126 (2004) 4581–4595.
[35] A. Blanc, C.G. Bochet, J. Org. Chem. 67 (2002) 5567–5577.
[36] C. Bochet, Angew. Chem. Int. Ed. 40 (2001) 2071–2073.
[37] A. Blanc, C.G. Bochet, Org. Lett. 9 (2007) 2649–2651.
[38] M.J. Frisch, G.W. Trucks, H.B. Schlegel, G.E. Scuseria, M.A. Robb, J.R. Cheeseman, G. Scalmani, V. Barone, B. Mennucci, G.A. Petersson, H. Nakatsuji, M. Caricato, X. Li, H.P. Hratchian, A.F. Izmaylov, J. Bloino, G. Zheng, J.L. Sonnenberg, M. Hada, M. Ehara, K. Toyota, R. Fukuda, J. Hasegawa, M. Ishida, T. Nakajima, Y. Honda, O. Kitao, H. Nakai, T. Vreven, J.A. Montgomery Jr., J.E. Peralta, F. Ogliaro, M. Bearpark, J.J. Heyd, E. Brothers, K.N. Kudin, V.N. Staroverov, R. Kobayashi, J. Normand, K. Raghavachari, A. Rendell, J.C. Burant, S.S. Iyengar, J. Tomasi, M. Cossi, N. Rega, J.M. Millam, M. Klene, J.E. Knox, J.B. Cross, V. Bakken, C. Adamo, J. Jaramillo, R. Gomperts, R.E. Stratmann, O. Yazyev, A.J. Austin, R. Cammi, C. Pomelli, J.W. Ochterski, R.L. Martin, K. Morokuma, V.G. Zakrzewski, G.A. Voth, P. Salvador, J.J. Dannenberg, S. Dapprich, A.D. Daniels, Ö. Farkas, J.B. Foresman, J.V. Ortiz, J. Cioslowski, D.J. Fox, Gaussian 09, Gaussian, Inc., Wallingford, CT, 2009.
[39] R. Stratmann, G. Scuseria, M. Frisch, J. Chem. Phys. 109 (1998) 8218–8224.
[40] G.A. Zhurko, D.A. Zhurko, ChemCraft, Pilmus Inc., Milpatas, CA, 2007.
[41] W.L.P. Armarego, D.D. Perrin, Purification of Laboratory Chemicals, Pergamon Press Inc., Elmsford, NY, 1998.
[42] O. Miyata, T. Koizumi, H. Asai, R. Iba, T. Naito, Tetrahedron 60 (2004) 3893–3914.
[43] A.S. Singha, B.N. Misra, Indian J. Chem. 21B (1982) 361–363.
[44] A. Gissot, A. Volonterio, M. Zanda, J. Org. Chem. 70 (2005) 6925–6928.
[45] O. Brady, F. Peakin, J. Chem. Soc. (1930) 226–229.
[46] P. Mamalis, J. Green, D. Mchale, J. Chem. Soc. (1960) 229–238.
[47] N.J. Bunce, J. LaMarre, S.P. Vaish, Photochem. Photobiol. 39 (1984) 531–533.
[48] M. Schworer, J. Wirz, Helv. Chim. Acta 84 (2001) 1441–1458.
[49] R. Yip, Y. Wen, D. Gravel, R. Giasson, D. Sharma, J. Phys. Chem. 95 (1991) 6078–6081.
[50] D. Gravel, R. Giasson, D. Blanchet, R. Yip, D. Sharma, Can. J. Chem. 69 (1991) 1193–1200.
[51] R. Yip, D. Sharma, R. Giasson, D. Gravel, J. Phys. Chem. 89 (1985) 5328–5330.
[52] R. Yip, D. Sharma, R. Giasson, D. Gravel, J. Phys. Chem. 88 (1984) 5770–5772.
[53] L. Hviid, J.W. Verhoeven, A.M. Brouwer, M.N. Paddon-Row, J. Yang, Photochem. Photobiol. Sci. 3 (2004) 246–251.
[54] D.E. Falvey, C. Sundararajan, Photochem. Photobiol. Sci. 3 (2004) 831–838.
[55] N. Turro, V. Ramamurthy, W. Cherry, W. Farneth, Chem. Rev. 78 (1978) 125–145.
[56] S.L. Murov, I. Carmichael, G.L. Hug, Handbook of Photochemistry, second ed., Marcel Dekker Inc., New York, NY, 1993.
[57] R. Finnegan, D. Knutson, J. Am. Chem. Soc. 90 (1968) 1670–1671.
[58] N. Turro, Modern Molecular Photochemistry, University Science Books, Sausalito, CA, 1991 (Chapter 6).